HHS Public Access

Author manuscript

Biochemistry. Author manuscript; available in PMC 2018 April 11.

Published in final edited form as:

Biochemistry. 2016 October 25; 55(42): 5927–5937. doi:10.1021/acs.biochem.6b00704.

Structures of the *Streptococcus sanguinis* SrpA Binding Region with Human Sialoglycans Suggest Features of the Physiological Ligand

Lioudmila V. Loukachevitch[$], **Barbara A. Bensing**[†], **Hai Yu**[#], **Jie Zeng**[#,^], **Xi Chen**[#], **Paul M. Sullam**[†], and **T M Iverson**[$,%,&,@,*]

[$]Department of Pharmacology, Vanderbilt University, Nashville, Tennessee 37232, USA

[%]Department of Biochemistry, Vanderbilt University, Nashville, Tennessee 37232, USA

[&]Center for Structural Biology, Vanderbilt University, Nashville, Tennessee 37232, USA

[@]Vanderbilt Institute of Chemical Biology, Vanderbilt University, Nashville, Tennessee 37232, USA

[†]Division of Infectious Diseases, Veterans Affairs Medical Center, University of California at San Francisco and the Northern California Institute for Research and Education, San Francisco, California 94121, USA

[#]Department of Chemistry, University of California, Davis, CA 95616, USA

[^]School of Food Science, Henan Institute of Science and Technology, Xinxiang, 453003, China

Abstract

Streptococcus sanguinis is a leading cause of bacterial infective endocarditis, a life threatening infection of heart valves. *S. sanguinis* binds to human platelets with high avidity, and this adherence is likely to enhance virulence. Previous studies suggest that a serine-rich repeat adhesin termed SrpA mediates the binding of *S. sanguinis* to human platelets via its interaction with sialoglycans on the receptor GPIbα. However, *in vitro* binding assays between SrpA and defined sialoglycans failed to identify specific high-affinity ligands. To better understand the interaction between SrpA and human platelets, we determined cocrystal structures of the SrpA sialoglycan binding region ($SrpA_{BR}$) with five low-affinity ligands: three sialylated trisaccharides (sialyl-T antigen, 3'-sialyllactose, and 3'-sialyl-*N*-acetyllactosamine), a sialylated tetrasaccharide (sialyl-$Lewis^X$) and a sialyl galactose disaccharide component common to these sialoglyans. We then combined structural analysis with mutagenesis to further determine whether our observed interactions between $SrpA_{BR}$ and glycans are important for binding to platelets and to better map the binding site for the physiological receptor. We found that the sialoglycan binding site of

[*]**Corresponding Author** To whom correspondence should be addressed: tina.iverson@vanderbilt.edu.

Author Contributions LVL performed crystallization and collected diffraction data; BAB performed site-directed mutagenesis, binding assays, and data analysis; HY and JZ synthesized sialyl T-antigen and the Neu5Ac-galactose disaccharide under the direction of XC; PS analyzed data; TMI determined the structures, performed crystallographic refinement, and analyzed the data. The manuscript was written through contributions of all authors. All authors have given approval to the final version of the manuscript.

PDB coordinates and structure factors have been deposited with the RCSB protein data bank (www.rcsb.org/pdb) with accession codes 5IIY, 5IJ1, 5IJ2, 5IJ3, and 5KIQ.

$SrpA_{BR}$ is significantly larger than the sialoglycans cocrystallized in this study, which suggests that SrpA binding to platelets is either multivalent or occurs via a larger, disialylated glycan.

INTRODUCTION

Serine-rich repeat (SRR) adhesins are cell wall anchored glycoproteins of streptococci and staphylococci that mediate adherence of the organism to proteins or glycans[1]. These interactions may be critical for commensal or pathogenic bacteria to attach to host tissues, and have been shown to enhance virulence[2–7]. The SRR adhesins contain ligand-binding domains that can fold independently and are highly variable in both their sequences and ligand repertoires. The differing specificities of the SRR adhesins for host receptors could explain the tropisms of the associated pathogens for specific tissues or anatomical sites.

Viridans group streptococci are a major cause of bacterial infective endocarditis[8, 9]. Attachment of the organism to platelets is a required step in the pathogenesis of this infection[10, 11], and many streptococcal strains express SRR adhesins that mediate binding to sialoglycans on platelet glycoprotein GPIb[2, 4, 12–14]. Among the best-studied sialoglycan-binding adhesins are SrpA from *Streptococcus sanguinis* strain SK36, GspB from *Streptococcus gordonii* strain M99, and Hsa from *S. gordonii* strain Challis (Fig. 1). SrpA, GspB, and Hsa can each mediate streptococcal adherence to carbohydrates on human platelets via a conserved sialoglycan binding region (BR) termed $SrpA_{BR}$, $GspB_{BR}$, and Hsa_{BR}, respectively[2, 4, 15]. The BRs of these three adhesins are clear homologs, with $SrpA_{BR}$ 32% identical to the corresponding region of $GspB_{BR}$[15] and 51% identical to Hsa_{BR}[3]. However, there are major differences in the carbohydrate-binding spectrum of SrpA, GspB, and Hsa[16]. GspB, which is expressed by a human endocarditis isolate and contributes to virulence in animal models of this disease, has nanomolar affinity for platelets[4] and binds a very narrow range of sialoglycans[16]. Hsa was cloned from an oral isolate[3] and similarly exhibits nanomolar affinity to human platelets[4] and a broad range of human sialoglycans[17]. SrpA was also identified in an oral isolate, and binds to platelets with similar avidity as GspB and Hsa[12, 14], suggesting a high-affinity interaction. As compared with these adhesins, however, SrpA appears to have markedly lower affinity for the defined sialoglycans that have been tested to date[16]. These data indicate that the specific sialoglycan attached to the GPIb receptor and recognized by SrpA has yet to be identified.

In recent work, we combined X-ray crystallography with functional binding measurements to identify the structural basis for sialoglycan binding by both $SrpA_{BR}$[18] and $GspB_{BR}$[19, 20]. These studies included a high-resolution costructure of $SrpA_{BR}$ bound to a non-human *N*-glycolylneuraminic acid (Neu5Gc)-based sialyl galactoside disaccharide[18]. Here, we further explore the binding repertoire of $SrpA_{BR}$, using a range of Neu5Ac-based α2-3 linked sialoglycans that are low-affinity ligands: sialyl-T antigen (Neu5Acα2–3Galβ1–3GalNAc; Fig. 2A), 3'-sialyllactose (Neu5Acα2–3Galβ1–4Glc; Fig. 2B), 3'-sialyl-*N*-acetyllactosamine (3'-sialyllactosamine; Neu5Acα2–3Galβ1–4GlcNAc; Fig. 2C), sialyl-$Lewis^X$ (Neu5Acα2–3Galβ1–4(Fucα1–3)GlcNAc; Fig. 2D) and a sialyl galactose disaccharide that is common to these trisaccharides (Neu5Acα2–3Gal; the β-galactose form is shown in the crystal structure, Fig. 2E). These studies indicate that the binding region of SrpA differs

significantly from GspB and Hsa in its interactions with sialoglycans. Moreover, SrpA is likely to accommodate either multiple ligands or larger, more complex ligands, as compared to these homologs.

EXPERIMENTAL PROCEDURES

Sialoglycan reagents

Sialyl-T antigen[21] and sialyl galactose[22] were synthesized as described previously. We purchased 3'-sialyllactose (Santa Cruz Biotechnology), 3'-sialyllactosamine (Carbosynth), and sialyl-Lewis^X (Calbiochem).

Expression and Purification of $SrpA_{BR}$

$SrpA_{BR}$ was expressed and purified with significant modifications of our previously described procedure[18]. The $SrpA_{BR}$ was expressed with tandem N-terminal His_6 and maltose binding protein (MBP) tags, using the isopropyl β-D-1-thiogalactopyranoside (IPTG) inducible pSV278 vector and *E. coli* BL21(*DE3*). Cells were grown in Terrific Broth at 37 °C until an OD_{600} of 2.0 was reached. The cells were then cooled on ice for 20 min, after which time expression was induced with 0.5 mM of IPTG. $SrpA_{BR}$ was expressed at 18 °C for 24 hrs. Cells were harvested by centrifugation, washed with Tris-HCl buffer (pH 7.5, 0.1 M) and pellets were stored at −20 °C before use. Frozen pellets were resuspended in binding buffer (50 mM Tris-HCl pH 7.5, 150 mM NaCl) containing PMSF (1 mM), leupeptin (2 μg/mL), pepstatin (2 μg/mL) and cells were lysed by sonication. The lysate was clarified by centrifugation at 38,500 × g for 40 min. His_6-MBP-tagged $SrpA_{BR}$ was purified at 4 °C on Ni-NTA agarose resin (Qiagen) using a batch procedure by adding Ni-NTA agarose resin to clarified lysate, incubating for 2 hrs, washing with binding buffer, and eluting tagged protein with binding buffer containing imidazole (250 mM). The eluted protein was concentrated in a 10 kDa MW cut-off concentrator and exchanged into binding buffer. The His_6-MBP affinity tag was cleaved with thrombin, and the cleaved affinity tag was separated from $SrpA_{BR}$ by a passage over Ni-NTA agarose column equilibrated with the binding buffer.

Crystallization and Structure Determination

$SrpA_{BR}$ (16 mg/mL in 20 mM Tris-HCl, pH 7.2) was mixed with sialyl-T antigen, 3'-sialyllactose, 3'-sialyllactosamine, sialyl-Lewis^X, or the disaccharide sialyl galactose and incubated on ice for 1 hr prior to crystallization. Cocrystals of $SrpA_{BR}$ with each sialoglycan were grown using the sitting drop vapor diffusion method in CombiClover 4 Chamber plates at room temperature (~23 °C) by equilibrating droplets containing 1 μL of protein-sialoglycan complex (14.4 mg/mL $SrpA_{BR}$, 10 mM sialoglycan, 18 mM Tris-HCl, pH 7.2) and 1μL of reservoir solution over a reservoir solution (50 μL) that contained $Ca(CH_3CO_2)_2$ (0.2 M), sodium cacodylate, pH 6.5 (0.1 M) and PEG 8000 (18%). Crystals were cryoprotected in reservoir solution containing 5 mM sialoglycan and cryocooled by plunging into liquid nitrogen. Data were collected at −180 °C on a MARCCD detector at LS-CAT ID-G at the Advanced Photon Source, processed using the HKL Suite[23], and converted with the CCP4 suite[24] (Table 1).

Cocrystals of $SrpA_{BR}$ with each sialoglycan were isomorphous with the unliganded structure. As a result, all structures were determined by removing solvent molecules from the unliganded $SrpA_{BR}$ structure (PDB entry 5EQ2[18]) and transferring the coordinates directly into each data set. Each model was subjected to an initial round of rigid body refinement in Phenix[25]. Sialoglycans were placed into the model after this initial structure determination and were retained at an occupancy of 1.0 during the course of the refinement process. Refinement proceeded using iterative rounds of Coot[26] and Phenix[25] until the R_{free} and the geometry was considered reasonable for each model (Table 2).

Binding of GST-tagged BRs to Platelet Monolayers

The production of glutathione *S*-transferase (GST)-tagged $SrpA_{BR}$ variants and the binding of GST-tagged BRs to platelet monolayers by ELISA were performed as previously described[27]. SrpA variant proteins were validated as stably folded using two complementary methods. First, we monitored degradation and chaperone-association using SDS-PAGE, where the chaperone-associated behavior identifies proteins that have exposed hydrophobic regions, and lowered stability. Second, we monitored monodispersity using size exclusion chromatography, where proteins with reduced stability will exhibit polydispersity, as reflected by a broadening of the peak width (not shown). Variants that exhibited either chaperone-associated behavior or polydispersity were not used for further analysis. Only variants that lacked chaperone-associated behavior and exhibited monodispersity were considered to be stably folded and were used in the assays.

Binding of platelet GPIbα to immobilized GST-$SrpA_{BR}$ and GST-$GspB_{BR}$

GST or GST-BR fusion proteins were diluted to 500 nM in PBS and 50 μL applied to microtiter wells. Plates were incubated 18 hr at 4°C. Unbound proteins were removed by aspiration, and wells were rinsed with 100 μL TEN buffer (10 mM Tris, 1 mM EDTA, 100 mM NaCl, pH 8). An extract enriched for glycocalicin (the soluble extracellular domain of GPIbα) was prepared by sonication of washed human platelets, followed by incubation at 37°C for 1 h to allow the proteolytic cleavage of GPIbα and release of glycocalicin, as described.[28] Insoluble debris was removed by centrifugation, followed by passage of the platelet extracts through a 0.45 μm filter. The platelet proteins were diluted to 60 μg/mL in TEN buffer containing Complete protease inhibitors (Roche) and 1X Blocking Reagent (Roche), with subsequent four-fold dilutions in the same buffer. Diluted platelet lysates (50 μL) were added to wells, and plates were incubated at 23 °C for 1 h with vigorous rocking. Wells were washed three times with PBS, and bound GPIbα was detected by ELISA, using a rabbit monoclonal anti-CD42b (abcam), followed by a peroxidase-conjugated goat anti-rabbit IgG (Sigma), and colorimetric detection with *o*-phenylenediamine (Sigma). The negative control was background subtracted from the measurements.

RESULTS

Relative binding of $SrpA_{BR}$ to platelets

A K_D value for the interaction between SrpA and platelet receptors has not been reported. However, SrpA has previously been implicated as mediating the attachment of *S. sanguinis* to platelet GPIbα at levels that are roughly comparable to the binding of *S. gordonii* strain

M99, which binds via an interaction between GspB and GPIbα, with a reported affinity of 23.8 nM[4]. We therefore used an ELISA assay to compare the relative binding of purified GST-tagged $SrpA_{BR}$ or purified GST-tagged $GspB_{BR}$ to intact platelets (Fig. 3A) or GPIbα in platelet lysates (Fig. 3B) over a range of concentrations. These studies showed that $SrpA_{BR}$ binds to intact platelets more strongly than does $GspB_{BR}$ under the conditions tested (Fig. 3A). Moreover, the interaction is clearly mediated by the GPIbα glycoprotein, with $SrpA_{BR}$ exhibiting ~10-fold higher avidity for GPIbα than $GspB_{BR}$ (Fig. 3B).

Structure of $SrpA_{BR}$ with Neu5Ac-based trisaccharides

To explore a range of low-affinity ligands that likely exhibit specific binding to SrpA, we focused on α2-3 linked Neu5Ac-based sialoglycans. In all of these sialoglycans, the identity and the linkage of the first two sugars are identical (Neu5Acα2-3Galβ), with variability in the identity and the linkage to the third sugar in the larger glycans, and the presence of a fourth sugar in sialyl-Lewis^X. Our studies included two trisaccharides known to decorate platelets (sialyl-T antigen (Fig. 2A), 3'-sialyllactosamine (Fig. 2C)) and the sialyl galactose disaccharide (Fig. 2E). We additionally examined the interaction with two low-affinity ligands not reported to be associated with platelets (3'-sialyllactose (Fig. 2B) and sialyl-Lewis^X (Fig. 2D)). The rationale for evaluating the trisaccharides that have not been found on platelets is that these can still provide insights as to the chemical properties of the physiological receptor.

We determined the high-resolution X-ray crystal structures of $SrpA_{BR}$ in complex with sialyl-T antigen, 3'-sialyllactose, 3'-sialyllactosamine, sialyl-Lewis^X and the sialyl galactose disaccharide (Fig. 4, Tables 1&2). Following isomorphous replacement, unambiguous electron density for each sialoglycan was readily apparent (Fig. 5, Table 3). For all the sialoglycans, the subjective quality of the electron density was the most unambiguous for the sialic acid. Moreover, with the exception of 3'sialyllactosamine, the contour level of the electron density where the hexose ring of each carbohydrate was associated with contiguous density was highest for the sialic acid (Table 3). This is consistent with the many direct hydrogen-bonding interactions between Neu5Ac and $SrpA_{BR}$. The hydrogen bonds involve the side chains of Gln 344, Thr 346, and Arg 347 (Fig. 6–9) and the main chain carbonyls of Arg 342 and Gln 344 (Fig. 8). Validating this binding mode, we previously showed that Thr 346 and Arg 347 are important for the interaction between SrpA and platelets via site-directed mutagenesis[18]. The electron densities for additional sugars were almost universally weaker (Fig. 5, Table 3), but were consistent with favorable conformations of each sialoglycan. For the trisaccharides and sialyl-Lewis^X (Fig. 5A–D), elaborations on both the galactoside and the third sugar could be observed in the initial electron density when contoured at or below 2σ. For the sialyl galactose disaccharide, the electron density of the galactose was quite weak and could only be observed when contoured below 2σ even after refinement, suggesting mobility of the galactose (Fig. 5E). The quality of the electron density for the galactose in the context of the disaccharide was subjectively worse than the quality of the electron density for galactoside in the context of the trisaccharides, suggesting that interactions between $SrpA_{BR}$ and the third sugar reduces the mobility of the galactoside.

As we previously observed for $SrpA_{BR}$ crystallized with a Neu5Gc-based sialyl galactoside disaccharide[18], only one of the protomers in the dimer was associated with clear electron density for sialoglycan ligand, with diffuse electron density apparent in the binding site in the second protomer of the dimer. Crystal packing interactions likely prevent binding of the ligand to the other binding site in the dimer, and previously-reported mutagenesis disrupting dimerization was not associated with changes in binding affinity[18], indicating no cooperativity between the sites. The single site sialoglycan binding to the dimer is depicted in Fig. 4.

Binding of di-, tri-, and tetrasaccharides to $SrpA_{BR}$ did not require backbone adjustments as compared to the unliganded structure, as evidenced by the rms deviation between sialoglycan-bound and unliganded $SrpA_{BR}$ ranging from 0.21 – 0.30 Å. A single side chain rotamer change, in Lys 296, accompanied glycan binding in the 3'-sialyllactosamine and sialyl-$Lewis^X$-bound SrpA. In each case, this made a weak hydrogen-bonding interaction with the third sugar; however the electron density suggested that this residue was somewhat mobile in all structures.

Differences in interaction between SrpA and Neu5Ac- or Neu5Gc-based sialoglycans

Naturally occurring sialic acid has different forms. Humans exclusively synthesize the *N*-acetylneuraminic acid (Neu5Ac) form; other animals also hydroxylate its nucleotide activated form, cytidine 5'-monophosphate-*N*-acetylneuraminic acid (CMP-Neu5Ac), on C11, resulting in the Neu5Gc form[29] (compare Fig. 2 E, F). Previous binding studies of SrpA to purified, defined glycans identified that SrpA preferentially binds the Neu5Gc form of sialic acid[16]. Comparison of the costructure of $SrpA_{BR}$ in complex with the Neu5Gc-based sialyl galactoside disaccharide[18] to each of the costructures of $SrpA_{BR}$ with each of the Neu5Ac-based sialyl galactose compounds identifies a favorable hydrogen-bonding interaction between the OH of Tyr 368 of $SrpA_{BR}$ and the unique hydroxyl of Neu5Gc (Fig. 6) that is absent in the Neu5Ac-based sialoglycans (Fig. 2A–E). This may explain the preference of SrpA for binding Neu5Gc. Attempts to verify this experimentally were unsuccessful due to the misfolding of site-directed variants, as indicated by evidence of protein degradation and co-purification with chaperones (not shown).

Sialoglycan interactions with SrpA

Interestingly, there are no direct hydrogen-bonding interactions between $SrpA_{BR}$ and the second, third, or fourth carbohydrate in any of the sialoglycans tested. Instead, these sugars exhibited two types of relatively non-selective interactions with SrpA. The first type of interaction between $SrpA_{BR}$ and these sialoglycans is achieved via positioning of an apical CH from the third sugar above the π-ring of Phe 294 (Fig. 7), which forms a stabilizing CH/π-stacking interaction. CH/π-stacking interactions are common in protein-carbohydrate interactions[30] and are proposed to promote weak facial selectivity for their ligands[31]. Notably, changing the linkage from 1➔3 (sialyl-T antigen) to 1➔4 (3'-sialyllactosamine, 3'-sialyllactosamine) and the identity of the sugar from *N*-acetylgalactosamine (GalNAc; sialyl-T antigen) to glucose (Glc; 3'-sialyllactose) or *N*-acetylglucosamine (GlcNAc; 3'-sialyllactosamine) is accompanied by a 180° rotation of the third sugar around the glycosidic linkage, which maintains the CH/π-stacking interaction. In comparison, the sialyl-$Lewis^X$

tetrasaccharide appears to be slightly rotated, which places the glycosidic linkage between the GlcNAc and the fucose (Fuc) above the Phe 294 tetrapole.

The second type of interaction between $SrpA_{BR}$ and the second and the third sugars of the trisaccharides is indirect, water molecule-mediated interactions (Fig. 8). The water-mediated hydrogen-bonding network extending from these sugars is extensive and structurally conserved in the costructures with all three trisaccharides (Fig. 8A–C) and only slightly altered with the sialyl-$Lewis^X$ tetrasaccharide (Fig. 8D). Close examination of this region identifies that the water molecule network extends through a shallow but extended surface cleft of $SrpA_{BR}$. While the functional relevance of this cleft has never been tested in SrpA, surface clefts of proteins are hallmarks of ligand-binding sites.[32] Interestingly, comparison of sialoglycan-bound $SrpA_{BR}$ or $GspB_{BR}$ to their unliganded counterparts identifies that positions occupied by hydroxyl groups of bound sialoglycans superimpose with water molecules in the unliganded structures. In considering this more extended water molecule network and the cleft adjacent to the bound trisaccharides, it appears that the available ligand-binding surface on the protein could be larger than required to accommodate a trisaccharide.

Molecular properties of the SrpA sialoglycan binding site

While the physiological sialoglycan ligand for SrpA remains unknown, structural comparison of SrpA with mammalian sialic acid binding immunoglobulin-like lectins (Siglec) offers one intriguing hypothesis. Mammalian Siglecs share a fold with SrpA and its bacterial homologs, but despite the similar fold, these two families of sialic acid binding proteins bind sialoglycans at distinct sites.[33–39] The bacterial homologs use the YTRY motif to anchor sialic acid above a strictly conserved arginine residue, which is Arg 347 in SrpA, Arg 484 in GspB, and Arg 340 in Hsa (Fig. 1). The mammalian Siglecs also bind at a conserved arginine (Arg 97 of Siglec-1 (sialoadhesin), Arg 124 of Siglec-5, or Arg 124 of Siglec-7, Fig. 9A), however this conserved mammalian arginine is not analogous to the bacterial arginine. Indeed, in a structural overlay of bacterial and mammalian Siglecs, the critical sialoglycan-binding arginines of each family are spatially separated by ~15 Å and appear to be parts of distinct sialoglycan binding pockets (Fig. 1, Fig. 9A–C). Although spatially separated, both the mammalian arginine and the bacterial arginine are located on the F-strand of the Ig fold.

Interestingly, SrpA appears to contain arginine residues corresponding to both a bacterial and a mammalian sialoglycan binding pocket (compare Fig. 9A–C); the bacterial sialoglycan-binding arginine of SrpA is Arg 347 and the mammalian-like sialoglycan-binding arginine is Arg 350 (Fig. 9B). SrpA is the first known example of either a mammalian or a bacterial Siglec that contains an arginine corresponding to the critical sialic acid binding residue of the other family. Indeed, the GspB and Hsa bacterial Siglecs that are homologs of SrpA do not have an arginine analogous to the mammalian sialoglycan binding arginine (Fig. 1).[19] In addition, the structure of $GspB_{BR}$ has been reported, and shows that the sialoglycan binding pocket is capped by a helix (Fig. 9C) that physically covers the mammalian binding site.[19]

If Arg 350 of SrpA were important for platelet binding, it could mean that a second, mammalian-like sialoglycan binding site is present in this bacterial adhesin, which suggests additional possibilities for the natural SrpA ligand. One possibility is that the mammalian- and bacterial sialoglycan binding sites of are connected so that SrpA can bind a larger and more complex sialoglycan ligand than has been previously tested, in particular a ligand that contains two sialic acids. A second possibility is that both the mammalian-like and bacterial-like binding cooperate to bind two glycans through a multivalent interaction.

Functional validation of SrpA residues required for platelet binding

To test which residues of the sialoglycan binding site in $SrpA_{BR}$ are important for binding to the physiological receptor, we assessed the impact of selected site-specific variations on the binding of purified $SrpA_{BR}$ to immobilized platelets (Fig. 10). First, we assessed the impact of mutating Phe 294, which would disrupt the CH/**π**-stacking interaction. Second, we assessed the impact of mutating Asn 361 and Thr 363, which contribute to the stabilization of the network of water-mediated hydrogen-bonding interactions between SrpA and each of the tri- and tetrasaccharides, but could also interact directly with a larger sialoglycan. Finally, we assessed the impact of mutating Arg 350, which does not interact either directly or indirectly with any of the trisaccharides or the sialyl-Lewis^X tetrasaccharide and is not conserved in bacterial Siglecs (Fig. 1), but which is analogous to the critical sialic acid-binding arginine of mammalian Siglecs. All variants folded correctly, as described in the experimental procedures (not shown). Moreover, the variants altered surface residues that are not conserved in SrpA homologs with different ligand specificity (Fig. 1), indicating that this domain can accommodate a range of amino acids at these positions. We compared the platelet binding of each variant to platelet binding exhibited by wild-type $SrpA_{BR}$ and the $SrpA_{BR}{}^{R347E}$ variant, a variant with the critical arginine of the bacterial YTRY sialic acid-binding motif altered. The $SrpA_{BR}{}^{R347E}$ variant has previously been demonstrated to significantly reduce platelet binding while retaining a folded structure[27], thus allowing it to serve as a control.

$SrpA_{BR}{}^{F294A}$, designed to disrupt CH/**π**-stacking, exhibited a modest but statistically significant reduction in platelet binding as compared to wild-type $SrpA_{BR}$. $SrpA_{BR}{}^{T363A}$ and $SrpA_{BR}{}^{N361A}$, designed to disrupt either the water molecule network or interactions to a larger physiological ligand, exhibited different effects on platelet binding. $SrpA_{BR}{}^{T363A}$ was associated with platelet binding that was only slightly reduced, as compared to wild-type $SrpA_{BR}$. In contrast, $SrpA_{BR}{}^{N361A}$ showed a substantial reduction in binding to platelets. The $SrpA_{BR}{}^{R350E}$ variant, designed to eliminate the mammalian-like sialoglycan-binding arginine, also displayed substantial loss of binding as compared to wild-type $SrpA_{BR}$. These mutagenesis studies identify Asn 361 and Arg 350 as important for high-affinity binding to platelet receptors. As previous studies identified both Thr 346 and Arg 347 to be key for platelet binding, and as Thr 346, Arg 347, Asn 361 and Arg 350 lie along a contiguous surface, the most reasonable interpretation of these results is that the functional SrpA receptor-binding pocket is much larger than is necessary to accommodate the ligands tested here (Fig. 9B). The features of this binding region could either be interpreted as two separate binding pockets for trisaccharides, or as a single binding pocket that binds a larger, more complex glycan.

DISCUSSION

The nature of the physiological sialoglycan receptor of SrpA during endocarditis

SrpA has been demonstrated to bind to human platelet GPIb[18], a highly sialylated glycoprotein. Moreover, SrpA contains strong sequence identity to GspB and Hsa[40], which both exhibit sialidase-sensitive platelet binding properties[41]. The sequence identity between SrpA, GspB, and Hsa extends to a loosely conserved YTRY sequence motif that binds to sialic acid (Fig. 1). The sequence is FTRT in SrpA[40]. The central Thr-Arg residues of this motif (Thr 346 and Arg 347) have been shown to be critical for platelet binding by SrpA, and these side chains directly interact with sialic acid in the crystal structures[18]. However, a defined high-affinity ligand for SrpA has not, to date, been identified[16].

Both the sialyl-T antigen and 3'-sialyllactosamine tested in these studies are known to decorate platelets; however, the full repertoire of platelet glycans is not known at this time, which hinders efforts to identify the receptor. Here, we identified two additional surface residues, Asn 361 and Arg 350, that are distal to the FTRT sequence and that impact SrpA affinity to platelets (Fig. 10). Asn 361 and Arg 350 are on a surface of SrpA that also contains the FTRT sequence (Fig. 9B), with the two arginines (Arg 347 and Arg 350) separated by ~15 Å. This receptor-binding surface in SrpA appears significantly larger than sialyl-T antigen-binding pocket on the GspB homolog (Fig. 9C).

One interpretation of these data is that SrpA improves affinity to platelets via a multivalent interaction, where SrpA simultaneously binds one sialoglycan above Arg 347 and a second sialoglycan (or another ligand) above Arg 350 (Fig. 11A). In this model, the two sialoglycans would be adjacent on the GPIb receptor. If this were the case, it might be anticipated that two glycans would bind to SrpA during crystallization. However, crystal contacts closely approach Arg 350, which would prevent a ligand from binding at this site. As a result, the lack of observed sialoglycan binding near Arg 350 in these crystal structures does not rule out the possibility of a multivalent interaction.

An alternative would be that SrpA binds a larger glycan (Fig. 11B) that interacts with both Arg 347 and Arg 350 simultaneously. Consistent with this second mechanism, both the mammalian-like Arg 350 and the bacterial-like Arg347 in SrpA are located on the F-strand of the Ig fold[19] and are arranged in a way that they could be a part of the same binding site. If SrpA does bind to a larger glycan during endocardial infection, the identity of this ligand is not immediately apparent because the full repertoire of sialoglycans present on platelets or GPIb is not well characterized.

One possibility could include sulfate elaborations of sialoglycans. Although not reported on GPIb to date, experimental support for a role of sulfated sialoglycans in binding comes from studies using sialoglycan arrays[16]. These arrays showed that sulfated substitutions of di- and trisaccharide sialoglycans bind to SrpA with similar or slightly increased affinity as compared to the non-sulfated versions[16].

Other possibilities for the true receptor are longer core 1 structures, and branched core 2 structures, potentially disialylated. Previous studies of the platelet glycoprotein GPIbα

identified a core 2 hexasaccharide comprised of sialyl-T antigen with β1–6 glycosidic linkage between the GlcNAc in 3'-sialyllactosamine Siaα2–3Galβ1–4GlcNAc and the core GalNAc in the sialyl-T antigen[42, 43] (this structure is shown in the conceptual model in Fig. 11B). This branched core 2 structure was reported to be the most abundant *O*-linked glycan on platelet GPIbα. If this disialylated hexasaccharide adopted an elongated conformation, its two sialic acids would be separated by ~15 Å, a distance ideal for interaction with Arg 347 and Arg 350. The central part of the glycan could then interact with Asn 361. This hexasaccharide is not readily available, making it difficult to experimentally validate this possibility at the present time.

Within these candidates for the SrpA receptor in humans, a Neu5Gc-containing sialoglycan cannot be excluded a priori. Although Neu5Gc is not synthesized in humans[29], there are some reports that low levels of Neu5Gc can be incorporated into the human glycan repertoire after absorption from dietary sources[44–46]. While there is no known correlation between a Neu5Gc-containing diet and endocardial infection caused by *S. sanguinis*, the observed additional hydrogen-bonding interaction between SrpA and Neu5Gc would suggest that a Neu5Gc-incorporated sialoglycan would be the preferred ligand over a Neu5Ac-incorporated sialoglycan.

Conclusions

Here, we determine that the SrpA adhesin contains a larger ligand binding surface than is necessary to bind a trisaccharide. This surface contains residues critical for platelet binding, including Thr 346, Arg 347, Arg 350, and Asn 361. The ligand binding site appears to be a composite of the binding sites identified in the bacterial homolog GspB and the mammalian Siglecs, both of which bind to sialoglycans. These data allow the proposal of a model where SrpA binds with much higher affinity to human platelets than to synthetic trisaccharides either by recognizing multiple, adjacent sialoglycans (increasing affinity with multivalency), or by recognizing a much larger sialoglycan (increasing affinity with additional contacts).

ACKNOWLEDGMENT

We thank Ajit Varki and Wendy Thomas for insightful discussions during the course of manuscript preparation and Jarrod Smith for assistance with computational analysis. A portion of the experiments described here used the Vanderbilt PacVan biomolecular robotic crystallization facility, which was supported by NIH grant S10 RR026915. Use of the Advanced Photon Source, an Office of Science User Facility operated for the U.S. Department of Energy (DOE) Office of Science by Argonne National Laboratory, was supported by the U.S. DOE under Contract No. DE-AC02-06CH11357. Use of the LS-CAT Sector 21 was supported by the Michigan Economic Development Corporation and the Michigan Technology Tri-Corridor (Grant 085P1000817).

FUNDING INFORMATION This work was supported by the Department of Veterans Affairs, grants from the National Institutes of Health ((NIH); AI41513 to PS, and AI106987 to TMI/PMS), and a grant from the American Heart Association (14GRNT20390021 to TMI).

ABBREVIATIONS

SRR	serine-rich repeat
MBP	maltose binding protein
GST	glutathione S-transferase

BR	binding region

REFERENCES

[1]. Lizcano A, Sanchez CJ, Orihuela CJ. A role for glycosylated serine-rich repeat proteins in gram-positive bacterial pathogenesis. Mol Oral Microbiol. 2012; 27:257–269. [PubMed: 22759311]

[2]. Bensing BA, Lopez JA, Sullam PM. The Streptococcus gordonii surface proteins GspB and Hsa mediate binding to sialylated carbohydrate epitopes on the platelet membrane glycoprotein Ibalpha. Infect Immun. 2004; 72:6528–6537. [PubMed: 15501784]

[3]. Takahashi Y, Konishi K, Cisar JO, Yoshikawa M. Identification and characterization of hsa, the gene encoding the sialic acid-binding adhesin of Streptococcus gordonii DL1. Infect Immun. 2002; 70:1209–1218. [PubMed: 11854202]

[4]. Takamatsu D, Bensing BA, Cheng H, Jarvis GA, Siboo IR, Lopez JA, Griffiss JM, Sullam PM. Binding of the Streptococcus gordonii surface glycoproteins GspB and Hsa to specific carbohydrate structures on platelet membrane glycoprotein Ibalpha. Mol Microbiol. 2005; 58:380–392. [PubMed: 16194227]

[5]. Obert C, Sublett J, Kaushal D, Hinojosa E, Barton T, Tuomanen EI, Orihuela CJ. Identification of a Candidate Streptococcus pneumoniae core genome and regions of diversity correlated with invasive pneumococcal disease. Infect Immun. 2006; 74:4766–4777. [PubMed: 16861665]

[6]. Seifert KN, Adderson EE, Whiting AA, Bohnsack JF, Crowley PJ, Brady LJ. A unique serine-rich repeat protein (Srr-2) and novel surface antigen (epsilon) associated with a virulent lineage of serotype III *Streptococcus agalactiae*. Microbiology. 2006; 152:1029–1040. [PubMed: 16549667]

[7]. Siboo IR, Chambers HF, Sullam PM. Role of SraP, a Serine-Rich Surface Protein of *Staphylococcus aureus*, in binding to human platelets. Infect Immun. 2005; 73:2273–2280. [PubMed: 15784571]

[8]. Hoen B, Duval X. Clinical practice. Infective endocarditis. N Engl J Med. 2013; 368:1425–1433. [PubMed: 23574121]

[9]. Murdoch DR, Corey GR, Hoen B, Miro JM, Fowler VG Jr. Bayer AS, Karchmer AW, Olaison L, Pappas PA, Moreillon P, Chambers ST, Chu VH, Falco V, Holland DJ, Jones P, Klein JL, Raymond NJ, Read KM, Tripodi MF, Utili R, Wang A, Woods CW, Cabell CH. Clinical presentation, etiology, and outcome of infective endocarditis in the 21st century: the International Collaboration on Endocarditis-Prospective Cohort Study. Arch Intern Med. 2009; 169:463–473. [PubMed: 19273776]

[10]. Fitzgerald JR, Foster TJ, Cox D. The interaction of bacterial pathogens with platelets. Nat Rev Microbiol. 2006; 4:445–457. [PubMed: 16710325]

[11]. Thiene G, Basso C. Pathology and pathogenesis of infective endocarditis in native heart valves. Cardiovasc Pathol. 2006; 15:256–263. [PubMed: 16979032]

[12]. Kerrigan SW, Douglas I, Wray A, Heath J, Byrne MF, Fitzgerald D, Cox D. A role for glycoprotein Ib in *Streptococcus sanguis*-induced platelet aggregation. Blood. 2002; 100:509–516. [PubMed: 12091342]

[13]. Plummer C, Douglas CW. Relationship between the ability of oral streptococci to interact with platelet glycoprotein Ibalpha and with the salivary low-molecular-weight mucin, MG2. FEMS Immunol Med Microbiol. 2006; 48:390–399. [PubMed: 17069618]

[14]. Plummer C, Wu H, Kerrigan SW, Meade G, Cox D, Ian Douglas CW. A serine-rich glycoprotein of *Streptococcus sanguis* mediates adhesion to platelets via GPIb. Br J Haematol. 2005; 129:101–109. [PubMed: 15801962]

[15]. Takamatsu D, Bensing BA, Prakobphol A, Fisher SJ, Sullam PM. Binding of the streptococcal surface glycoproteins GspB and Hsa to human salivary proteins. Infect Immun. 2006; 74:1933–1940. [PubMed: 16495569]

[16]. Deng L, Bensing BA, Thamadilok S, Yu H, Lau K, Chen X, Ruhl S, Sullam PM, Varki A. Oral streptococci utilize a Siglec-like domain of serine-rich repeat adhesins to preferentially target platelet sialoglycans in human blood. PLoS Pathog. 2014; 10:e1004540. [PubMed: 25474103]

[17]. Takahashi Y, Takashima E, Shimazu K, Yagishita H, Aoba T, Konishi K. Contribution of sialic acid-binding adhesin to pathogenesis of experimental endocarditis caused by *Streptococcus gordonii* DL1. Infect Immun. 2006; 74:740–743. [PubMed: 16369032]

[18]. Bensing BA, Loukachevitch L, McCulloch KM, Vann K, Yu H, Chen X, Sullam PM, Iverson TM. Structural Basis for Sialylated Carbohydrate Binding by the *Streptococcus sanguinis* SrpA Adhesin. J Biol Chem. 2016

[19]. Pyburn TM, Bensing BA, Xiong YQ, Melancon BJ, Tomasiak TM, Ward NJ, Yankovskaya V, Oliver KM, Cecchini G, Sulikowski GA, Tyska MJ, Sullam PM, Iverson TM. A structural model for binding of the serine-rich repeat adhesin GspB to host carbohydrate receptors. PLoS Pathog. 2011; 7:e1002112. [PubMed: 21765814]

[20]. Pyburn TM, Yankovskaya V, Bensing BA, Cecchini G, Sullam PM, Iverson TM. Purification, crystallization and preliminary X-ray diffraction analysis of the carbohydrate-binding region of the *Streptococcus gordonii* adhesin GspB. Acta Crystallogr Sect F Struct Biol Cryst Commun. 2010; 66:1503–1507.

[21]. Lau K, Yu H, Thon V, Khedri Z, Leon ME, Tran BK, Chen X. Sequential two-step multienzyme synthesis of tumor-associated sialyl T-antigens and derivatives. Org Biomol Chem. 2011; 9:2784–2789. [PubMed: 21359399]

[22]. Yu H, Chokhawala H, Karpel R, Yu H, Wu B, Zhang J, Zhang Y, Jia Q, Chen X. A multifunctional Pasteurella multocida sialyltransferase: a powerful tool for the synthesis of sialoside libraries. J Am Chem Soc. 2005; 127:17618–17619. [PubMed: 16351087]

[23]. Otwinowski, Z, Minor, W. Processing of X-ray Diffraction Data Collected in Oscillation Mode. In: Carter, C, , JrSweet, R, editors. Methods in Enzymology. Academic Press; NewYork: 1997. 307–326.

[24]. Winn MD, Ballard CC, Cowtan KD, Dodson EJ, Emsley P, Evans PR, Keegan RM, Krissinel EB, Leslie AG, McCoy A, McNicholas SJ, Murshudov GN, Pannu NS, Potterton EA, Powell HR, Read RJ, Vagin A, Wilson KS. Overview of the CCP4 suite and current developments. Acta Crystallogr D Biol Crystallogr. 2011; 67:235–242. [PubMed: 21460441]

[25]. Adams PD, Afonine PV, Bunkoczi G, Chen VB, Davis IW, Echols N, Headd JJ, Hung LW, Kapral GJ, Grosse-Kunstleve RW, McCoy AJ, Moriarty NW, Oeffner R, Read RJ, Richardson DC, Richardson JS, Terwilliger TC, Zwart PH. PHENIX: a comprehensive Python-based system for macromolecular structure solution. Acta Crystallogr D Biol Crystallogr. 2010; 66:213–221. [PubMed: 20124702]

[26]. Emsley P, Cowtan K. Coot: model-building tools for molecular graphics. Acta Crystallogr D Biol Crystallogr. 2004; 60:2126–2132. [PubMed: 15572765]

[27]. Bensing BA, Loukachevitch LV, McCulloch KM, Yu H, Vann KR, Wawrzak Z, Anderson S, Chen X, Sullam PM, Iverson TM. Structural Basis for Sialoglycan Binding by the *Streptococcus sanguinis* SrpA Adhesin. J Biol Chem. 2016; 291:7230–7240. [PubMed: 26833566]

[28]. Yan R, Mo X, Paredes AM, Dai K, Lanza F, Cruz MA, Li R. Reconstitution of the platelet glycoprotein Ib-IX complex in phospholipid bilayer Nanodiscs. Biochemistry. 2011; 50:10598–10606. [PubMed: 22080766]

[29]. Varki A. Loss of N-glycolylneuraminic acid in humans: Mechanisms, consequences, and implications for hominid evolution. Am J Phys Anthropol. 2001; (Suppl 33):54–69.

[30]. Asensio JL, Arda A, Canada FJ, Jimenez-Barbero J. Carbohydrate-aromatic interactions. Acc Chem Res. 2013; 46:946–954. [PubMed: 22704792]

[31]. Santana AG, Jimenez-Moreno E, Gomez AM, Corzana F, Gonzalez C, Jimenez-Oses G, Jimenez-Barbero J, Asensio JL. A dynamic combinatorial approach for the analysis of weak carbohydrate/aromatic complexes: dissecting facial selectivity in CH/pi stacking interactions. J Am Chem Soc. 2013; 135:3347–3350. [PubMed: 23418701]

[32]. Laskowski RA, Luscombe NM, Swindells MB, Thornton JM. Protein clefts in molecular recognition and function. Protein Sci. 1996; 5:2438–2452. [PubMed: 8976552]

[33]. Zhuravleva MA, Trandem K, Sun PD. Structural implications of Siglec-5-mediated sialoglycan recognition. J Mol Biol. 2008; 375:437–447. [PubMed: 18022638]

[34]. Attrill H, Imamura A, Sharma RS, Kiso M, Crocker PR, van Aalten DM. Siglec-7 undergoes a major conformational change when complexed with the alpha(2,8)-disialylganglioside GT1b. J Biol Chem. 2006; 281:32774–32783. [PubMed: 16895906]

[35]. Attrill H, Takazawa H, Witt S, Kelm S, Isecke R, Brossmer R, Ando T, Ishida H, Kiso M, Crocker PR, van Aalten DM. The structure of siglec-7 in complex with sialosides: leads for rational structure-based inhibitor design. Biochem J. 2006; 397:271–278. [PubMed: 16623661]

[36]. Zaccai NR, May AP, Robinson RC, Burtnick LD, Crocker PR, Brossmer R, Kelm S, Jones EY. Crystallographic and in silico analysis of the sialoside-binding characteristics of the Siglec sialoadhesin. J Mol Biol. 2007; 365:1469–1479. [PubMed: 17137591]

[37]. Zaccai NR, Maenaka K, Maenaka T, Crocker PR, Brossmer R, Kelm S, Jones EY. Structure-guided design of sialic acid-based Siglec inhibitors and crystallographic analysis in complex with sialoadhesin. Structure. 2003; 11:557–567. [PubMed: 12737821]

[38]. Bukrinsky JT, St Hilaire PM, Meldal M, Crocker PR, Henriksen A. Complex of sialoadhesin with a glycopeptide ligand. Biochim Biophys Acta. 2004; 1702:173–179. [PubMed: 15488769]

[39]. Alphey MS, Attrill H, Crocker PR, van Aalten DM. High resolution crystal structures of Siglec-7. Insights into ligand specificity in the Siglec family. J Biol Chem. 2003; 278:3372–3377. [PubMed: 12438315]

[40]. Bensing BA, Khedri Z, Deng L, Yu H, Fisher SJ, Chen X, Iverson TM, Varki A, Sullam PM. Novel aspects of sialoglycan recognition by the Siglec-like domains of streptococcal SRR glycoproteins. Glycobiology. 2016

[41]. Jakubovics NS, Kerrigan SW, Nobbs AH, Stromberg N, van Dolleweerd CJ, Cox DM, Kelly CG, Jenkinson HF. Functions of cell surface-anchored antigen I/II family and Hsa polypeptides in interactions of *Streptococcus gordonii* with host receptors. Infect Immun. 2005; 73:6629–6638. [PubMed: 16177339]

[42]. Korrel SA, Clemetson KJ, van Halbeek H, Kamerling JP, Sixma JJ, Vliegenthart JF. Identification of a tetrasialylated monofucosylated tetraantennary N-linked carbohydrate chain in human platelet glycocalicin. FEBS Lett. 1988; 228:321–326. [PubMed: 3342888]

[43]. Korrel SA, Clemetson KJ, Van Halbeek H, Kamerling JP, Sixma JJ, Vliegenthart JF. Structural studies on the O-linked carbohydrate chains of human platelet glycocalicin. Eur J Biochem. 1984; 140:571–576. [PubMed: 6327299]

[44]. Bardor M, Nguyen DH, Diaz S, Varki A. Mechanism of uptake and incorporation of the non-human sialic acid N-glycolylneuraminic acid into human cells. J Biol Chem. 2005; 280:4228–4237. [PubMed: 15557321]

[45]. Alisson-Silva F, Kawanishi K, Varki A. Human risk of diseases associated with red meat intake: Analysis of current theories and proposed role for metabolic incorporation of a non-human sialic acid. Mol Aspects Med. 2016

[46]. Takahashi T, Takano M, Kurebayashi Y, Masuda M, Kawagishi S, Takaguchi M, Yamanaka T, Minami A, Otsubo T, Ikeda K, Suzuki T. N-glycolylneuraminic acid on human epithelial cells prevents entry of influenza A viruses that possess N-glycolylneuraminic acid binding ability. J Virol. 2014; 88:8445–8456. [PubMed: 24829344]

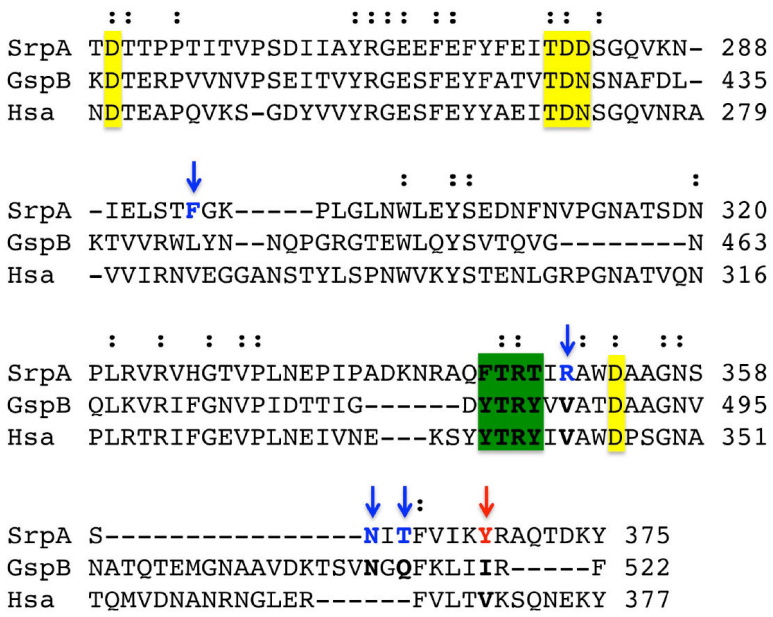

Figure 1.

Sequence alignment of the Siglec domain of SrpA, GspB, and Hsa. Residues conserved in all three homologs are marked with a colon (:). The YTRY sialic acid-binding motif is highlighted with a *green* box. As discussed in the text, this motif contains a conserved arginine residue (Arg 347 of SrpA, Arg 484 of GspB and Arg 340 of Hsa) that makes direct hydrogen-bonding interactions to the sialic acid. Additional key residues discussed in the text are highlighted with arrows. These include the putative Neu5Gc selectivity residue Tyr 368 (highlighted with a *red* arrow), and the putative glycan binding residues Phe 294, Arg 350, Asn 361, and Thr 363 (highlighted with a *blue* arrow). The cation binding residues are highlighted with *yellow* boxes.

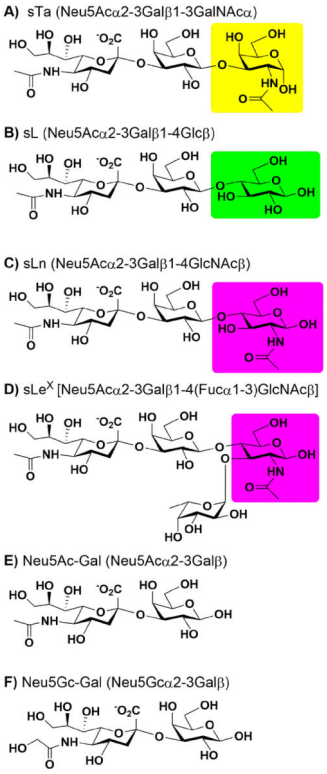

Figure 2.

Sialoglycans used in this study. (A) sialyl-T antigen (sTa), (B) 3'-sialyllactose (sL), (C) 3'-sialyllactosamine (sLn), (D) sialyl-Lewis^X (sLe^X), (E) Neu5Ac-Gal. (F) Neu5Gc-Gal. Shaded boxes highlighting the third sugar have the same color as the stick structures in Figs. 3, and 5 – 7.

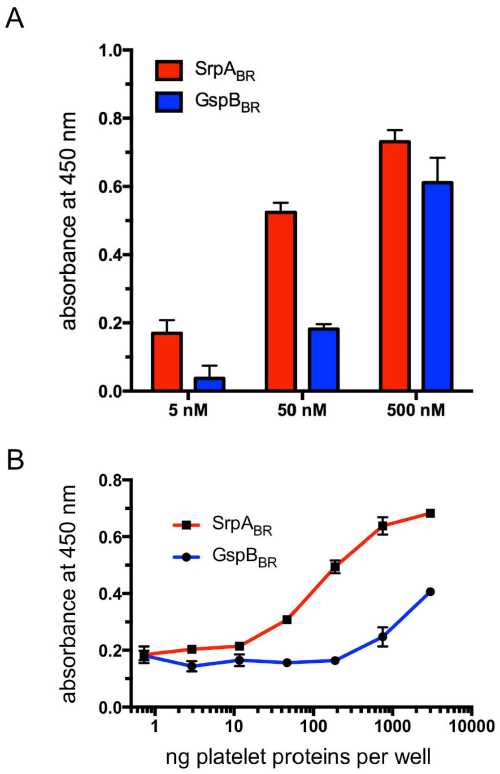

Figure 3.

Comparative binding of SrpA$_{BR}$ and GspB$_{BR}$ to human platelets or to platelet GPIbα. (A) Binding of GST-BRs (5–500 nM) to platelet monolayers. Measurements were background subtracted. (B) Binding of platelet GPIbα to immobilized GST-BRs. Data are reported as the mean ± standard deviation, with n=4.

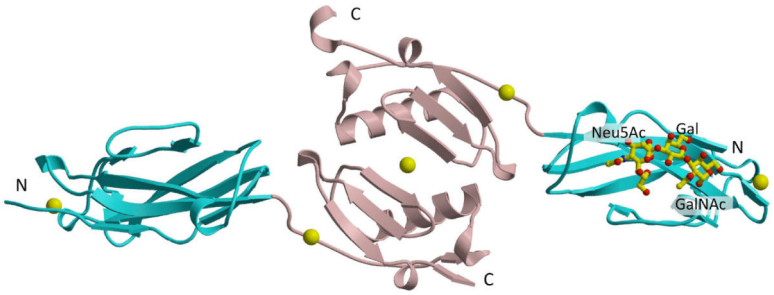

Figure 4.

Overview of a trisaccharide-bound $SrpA_{BR}$ dimer. The two polypeptide chains forming the dimer are depicted with the N-terminal Siglec domain colored cyan and the C-terminal Unique domain colored pink. Dimerization is mediated by the Unique domain. The sialyl-T antigen trisaccharide bound to the Siglec domain is shown in yellow sticks. Constraints of the crystal packing interactions likely result in the binding of only one sialoglycan molecule to the dimer. Divalent cations proposed to be physiologically relevant are shown as yellow spheres; additional ions from the crystallization conditions are not shown.

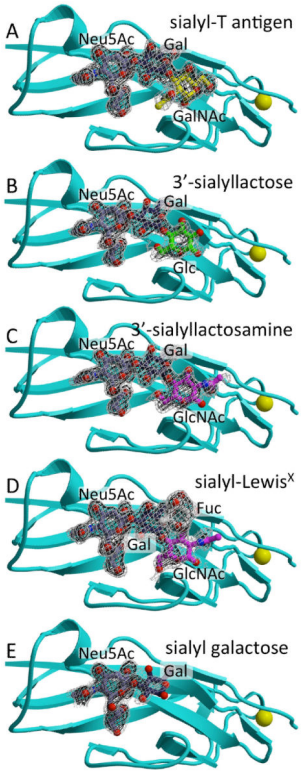

Figure 5.

Electron density for Neu5Ac-based sialylated trisaccharides binding to $SrpA_{BR.}$ (A) sialyl-T antigen (B) 3'-sialyllactose (C) 3'-sialyllactosamine (D) sialyl-Lewis^X (E) sialyl galactose. In each panel, $|F_o| - |F_c|$ electron density calculated after the removal of the sialoglycan and three cycles of refinement in Phenix[25] is contoured at 3σ (*black*) and 1.8σ (*white*) and is overlaid with the final model of the Siglec domain of each $SrpA_{BR}$ costructure. In all panels, the Neu5Ac is colored grey, the galactoside is colored navy, oxygens are colored red, and nitrogens are colored blue. For the trisaccharides, the third sugar differs in both identity and linkage and is colored *yellow* (1➔3GalNAc, sialyl-T antigen), *green* (1➔4 Glc, 3'-sialyllactose) or *magenta* (1➔4 GlcNAc, 3'-sialyllactosamine and sialyl-Lewis^X). The fucose of sialyl-Lewis^X (Fucα1➔3GlcNAc) is colored *white*.

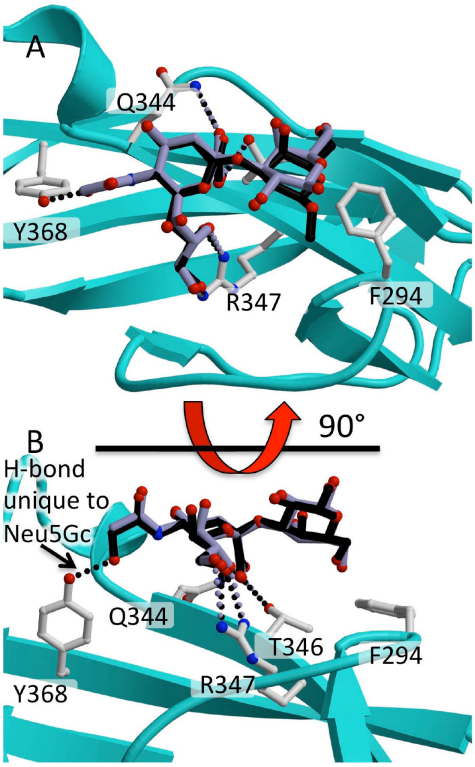

Figure 6.

A comparison of Neu5Ac and Neu5Gc-based disaccharides bound to $SrpA_{BR}$. The Neu5Gc-based sialyl galactoside disaccharide is shown in *black*, the Neu5Ac-based sialyl galactose disaccharide is shown in *lavender*, oxygens are colored *red*, and nitrogens are colored *blue*. Hydrogen bonding interactions have the same color as each disaccharide. The synthetic Neu5Gc-based sialyl galactose makes an additional hydrogen-bond to Tyr 368 as compared to the Neu5Ac-based glycans (*black* dotted line).

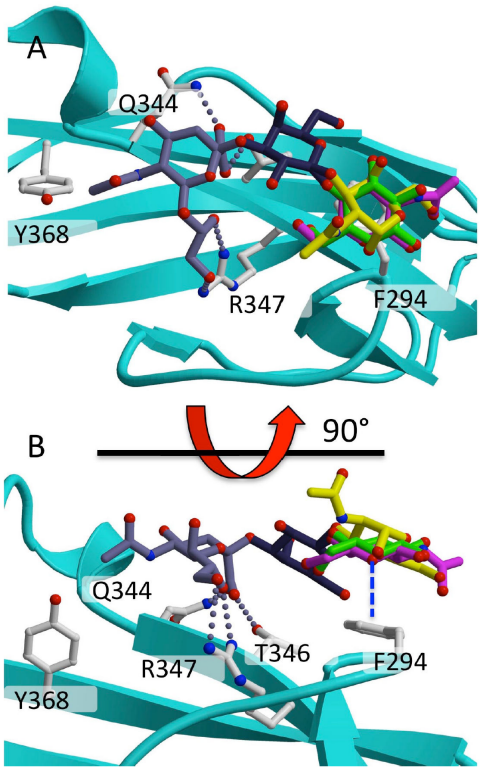

Figure 7.

Overlay of trisaccharides bound to $SrpA_{BR}$. The views in (A) and (B) are separated by 90°. The trisaccharides are colored as in Figure 5, with the conserved glycans (Neu5Ac, *grey*; Gal, *navy*) represented by the positions in sialyl-T antigen, and the direct hydrogen-bonding contacts between Neu5Ac and $SrpA_{BR}$ are the same in all three trisaccharides. Carbon atoms and bonds of the third sugar are colored *yellow* (sialyl-T antigen) *green* (3'-sialyllactose) or *magenta* (3'-sialyllactosamine), respectively. Oxygens are colored *red*, and nitrogens are colored *blue*. Direct interactions include both hydrogen-bonding interactions between the protein and the Neu5Ac, and a CH/π stacking interaction (*blue* dashed line) between the hexose ring of the third sugar and the side chain of Phe294.

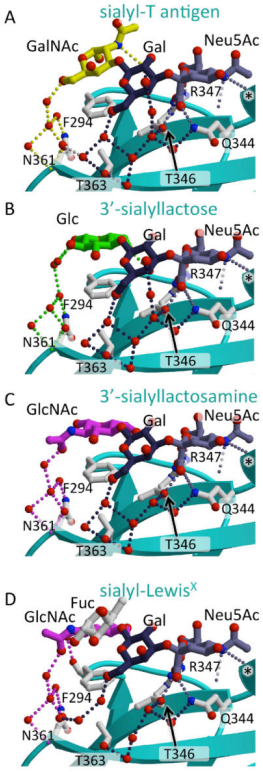

Figure 8.

Comparison of the direct and water mediated hydrogen-bonding interactions between $SrpA_{BR}$ and (A) sialyl-T antigen (B) 3'-sialyllactose (C) 3'-sialyllactosamine and (D) sialyl-Lewis^X. Direct hydrogen-bonding interactions between $SrpA_{BR}$ and the sialic acid are observed for all three sialoglycans (*light grey* dotted lines). Some hydrogen-bonding interactions involve backbone atoms; for example Arg 342 (discussed in the text) has an interaction to the backbone carbonyl. The Cα of Arg 342 is marked with a *. Water molecules (*red* spheres) form hydrogen-bonding interactions that bridge the galactoside to Gln 344/Thr 363/Thr 346 (*navy* dashed lines) and bridge the third sugar to Asn 361 (dotted lines colored similarly to the third sugar). No direct or indirect interactions to the fucose of sialyl-Lewis^X are observed. Minimal alteration in water molecule structure and hydrogen-bonding pattern is required to accommodate the different elaborations and linkages on the three trisaccharides (panels A–C). However, the rotation of sialyl-Lewis^X with respect to the remaining glycans alters the water molecule structure somewhat. The view is rotated 180° in the z-axis and 75° in the x-axis with respect to Figure 5; this view is rotated approximately 180° around the y-axis with respect to Figures 6B and 7B.

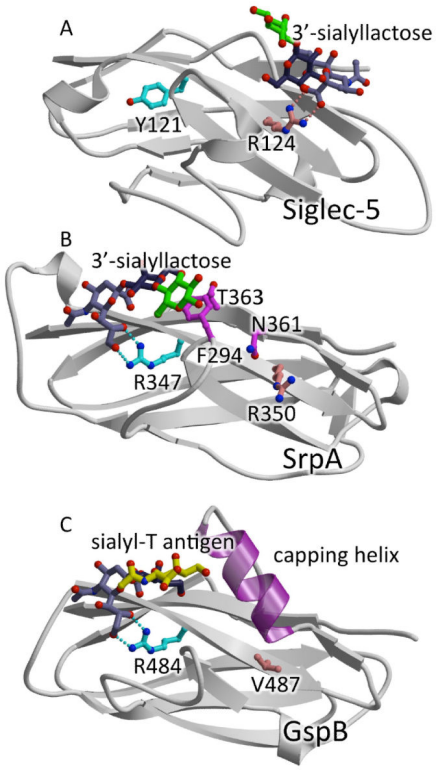

Figure 9.

The SrpA sialoglycan binding site has additional functional regions. (A) – (C) Side-by-side comparison of the isolated Siglec domain of (A) mammalian Siglec-5 bound to 3'-sialyllactose (PDB entry 2ZG3[33]) (B) SrpA bound to 3'-sialyllactose and (C) GspB bound to sialyl-T antigen (PDB entry 5IUC). Residues equivalent to Arg 347 and Arg 350 of SrpA are highlighted. The view is rotated by 30° in both the x- and y-axes as compared to the view in Fig. 3 in order to better observe both sialoglycan binding sites. (A) In mammalian Siglec-5, sialic acid binds forms two hydrogen-bonding interactions to Arg 124 (*pink*) on the F-strand of the V-set Ig fold. Tyr 121 (*cyan*) is observed in the same position as the sialic acid-binding arginine of SrpA and its homolog GspB. (B) In SrpA, the sialic acid binds to the FTRT sequence motif and forms two hydrogen-bonding interactions to Arg 347 on the F-strand (*cyan*), but also contains Arg 350, analogous to the sialic acid binding sequence of siglec-5 (*pink*). This second, putative sialic acid binding site is ~15 Å distal and is unoccupied in these structures, with crystal packing interactions occluding access to this region. Additional residues that were investigated by site-directed mutagenesis are highlighted in *magenta*. (C) In the SrpA homolog GspB, only the SrpA-like sialoglycan binding site is observed, and is organized around Arg 484 (*cyan*). Instead of a second arginine residue, GspB has Val 487 (*pink*) at this position. Moreover, a helix unique to GspB (*magenta*) is in the same location as the binding resides of siglec-5. This helix provides a defined boundary for the GspB binding pocket that limits the size of the glycan and blocks access to Val 487.

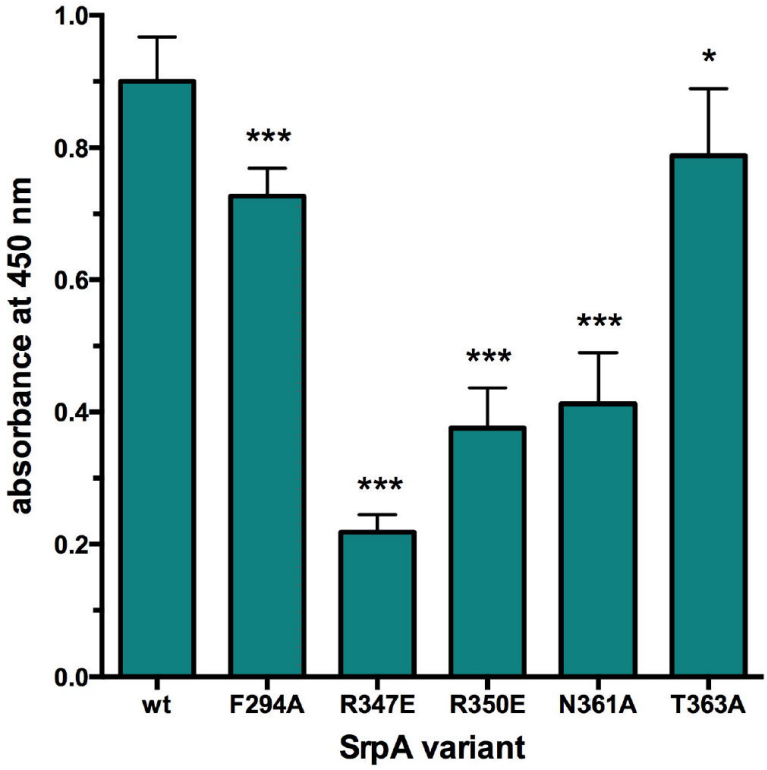

Figure 10.

Binding of N-terminally GST-tagged $SrpA_{BR}$ variants to platelet monolayers, as monitored by ELISA. Measurements were background subtracted for non-specific binding between GST and platelets. Measurements were performed in triplicate and are expressed as the mean ±S.D. All variants had binding that was significantly different from wild-type, as assessed as assessed by analysis of variance (ANOVA) combined with the Bonferroni multiple comparisons test, * $p \leq 0.02$, *** $p \leq 0.001$.

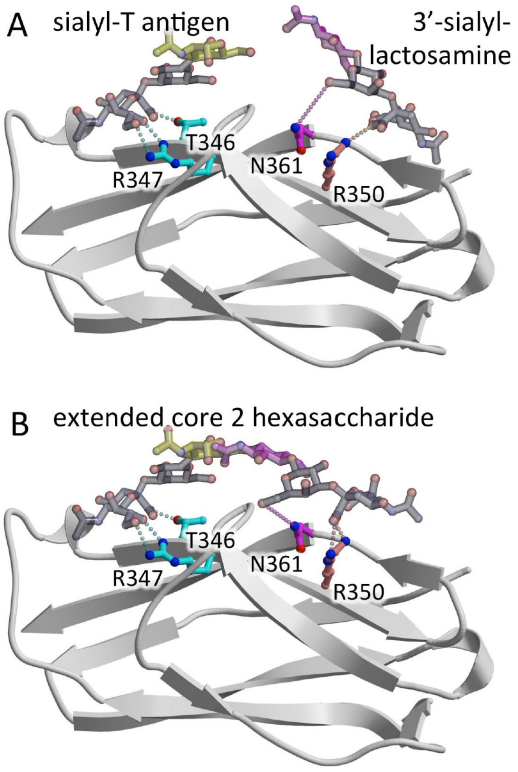

Figure 11.

Conceptual model for the binding of SrpA to platelet glycans. View is rotated 45° around the x-axis as compared to Fig. 9. Side chains that have a dramatic impact on platelet binding are shown as sticks. (A) Model for a multivalent interaction mode with sialyl-T antigen bound to the GspB-like binding site and 3'-sialyllactosamine bound to the mammalian-like binding site. (B) Model for an interaction with a larger, disialylated carbohydrate. Shown is the extended core 2 hexasaccharide Neu5Acα2–3Galβ1–3(Neu5Acα2–3Galβ1–4GlcNAcβ1–6)GalNAcα.

Table 1
Crystallographic data collection statistics

Raw diffraction data can be accessed using doi:10.15785/SBGRID/###, where ### indicates the SBGrid entry number listed above.

	sialoglycan bound to $SrpA_{BR}$				
	sialyl-T antigen	**3'-sialyllactose**	**3'-sialyllactosamine**	**3'-sialyl-galactose**	**sialyl-$Lewis^X$**
PDB entry	5IJ3	5IJ1	5IJ2	5IIY	5KIQ
SBGrid entry	244	245	246	247	326
Resolution	1.7 Å	1.8 Å	1.7 Å	1.9 Å	1.65 Å
APS Beamline	21-ID-G	21-ID-G	21-ID-G	21-ID-G	21-ID-F
Wavelength	0.979 Å	0.979 Å	0.979 Å	0.979 Å	0.979 Å
Space group	C2	C2	C2	C2	C2
Unit Cell	a=173.9 Å	a=174.5 Å	a=174.5 Å	a=174.5 Å	a=173.9 Å
	b=46.8 Å	b=46.8 Å	b=46.7 Å	b=46.8 Å	b=46.8 Å
	c=65.2 Å	c=64.8 Å	c=64.8 Å	c=64.8 Å	c=65.2 Å
	β=102.7°	β=102.7°	β=102.7°	β=102.7°	β=102.7°
R_{sym}	0.055 (0.460)	0.058 (0.475)	0.069 (0.572)	0.086 (0.552)	0.056 (0.686)
R_{pim}	0.022 (0.215)	0.032 (0.276)	0.033 (0.301)	0.042 (0.276)	0.027 (0.326)
$C_{1/2}$	0.889	0.833	0.690	0.881	0.863
I/σ	42.7 (4.0)	28.9 (3.1)	33.3 (2.5)	20.4 (2.6)	33.4 (2.5)
Completeness (%)	99.7 (97.0)	94.4 (64.0)[a]	97.8 (88.4)	97.6 (99.2)	99.2 (99.6)
Redundancy	7.1 (5.5)	4.2 (3.7)	5.5 (4.4)	4.8 (4.8)	5.0 (5.2)

[a]The completeness of the outer shell data (from 1.83–1.80 Å resolution) for the 3'-sialyllactose costructure was influenced by the geometry used during data collection. The data are 71.6% complete in the second to last resolution shell (1.86 – 1.83 Å resolution).

Table 2

Crystallographic refinement statistics.

	sialoglycan bound to $SrpA_{BR}$				
	sialyl-T antigen	**3'-sialyllactose**	**3'-sialyllactosamine**	**3'-sialyl-galactose**	**sialyl-Lewis^X**
PDB entry	5IJ3	5IJ1	5IJ2	5IIY	5KIQ
Resolution	1.7 Å	1.8 Å	1.7 Å	1.9 Å	1.65 Å
R_{cryst}	0.184	0.175	0.181	0.175	0.193
R_{free}	0.206	0.198	0.207	0.201	0.218
RMS deviation					
Bond lengths	0.005 Å	0.006 Å	0.012 Å	0.018 Å	0.012 Å
Bond angles	0.896°	1.190°	1.405°	0.894°	1.317°
Ramachandran					
Most favored	97.9 %	97.7 %	97.4 %	98.0%	97.7%
Additional	2.1 %	2.3 %	2.6 %	2.0%	2.3%
Disallowed	0.0 %	0.0 %	0.0 %	0.0%	0.0%
B factors					
Protein	26.1 $Å^2$	24.8 $Å^2$	25.0 $Å^2$	27.3 $Å^2$	32.8 $Å^2$
Glycan	35.0 $Å^2$	34.9 $Å^2$	38.2 $Å^2$	38.1 $Å^2$	45.8 $Å^2$

Table 3

Electron density of bound sialoglycans

Relative electron density contours where each sugar is associated with contiguous density. NA= not applicable.

	Carbohydrate position			
	1	**2**	**3**	**4**
Glycan	**(sialic acid)**	**(galactose)**	**(variable)**	**(fucose)**
sialyl-T antigen	6.0 σ	4.5 σ	4.0 σ	NA
3'-sialyllactose	4.0 σ	2.5 σ	2.5 σ	NA
3'-sialyllactosamine	3.5 σ	3.0 σ	5.0 σ	NA
3'sialyl galactose	4.0 σ	1.8 σ	NA	NA
sialyl-Lewis^X	5.0 σ	4.5 σ	2.0 σ	4.0 σ